Local spatio-temporal bedform patterns on an ebb-tidal delta

Laura Brakenhoff *Utrecht University, Utrecht, The Netherlands – l.b.brakenhoff@uu.nl*
Maarten van der Vegt *Utrecht University, Utrecht, The Netherlands – m.vandervegt@uu.nl*
Gerben Ruessink *Utrecht University, Utrecht, The Netherlands – b.g.ruessink@uu.nl*

ABSTRACT: Ebb-tidal deltas are highly complex areas, influenced by both waves and currents. The complex hydrodynamic situation creates an equally complex set of bedforms, varying in both space and time. The present study explores the presence and characteristics of bedforms on the Ameland ebb-tidal delta, which is located along the north coast of the Netherlands. Spatially extensive patterns were determined with a multibeam echosounder, whereas the development of bedforms through time in a limited spatial area was measured with a 3D profiling Sonar. It was found that the area seaward of the shoal consisted of a megaripple field, which disappeared after a storm. Within this area, 3D small-scale wave-current ripples were also found, which recovered within a few days after the storm.

1 INTRODUCTION

Ebb-tidal deltas are sand bodies located seaward of tidal inlets, and are therefore affected by both waves and currents, the latter comprising cross- and longshore tidal and wind-driven currents. The combined action of waves and currents creates a wide range of bedforms.

The largest bedforms on ebb-tidal deltas are sandy shoals, which have been studied thoroughly by, for example, FitzGerald (1982) and Ridderinkhof et al. (2016). In the Wadden Sea region, saw-tooth bars are often present on the downdrift side of ebb-tidal deltas, with heights up to 2 m and wavelengths (i.e. spacings) of about 700 m (Brakenhoff et al., 2018). Smaller bedforms like ripples and sand waves are also found on ebb-tidal deltas, but previous studies have only focused on these bedforms in channels and tidal inlets (e.g. Buijsman and Ridderinkhof, 2008). A more general overview of the presence and dynamics of these smaller scale bedforms is still lacking. Nevertheless, these bedforms affect bed roughness and therefore also flow and sediment transport. Thus, an accurate prediction of bedform characteristics is vital to improve the quality of sediment transport predictions, for example those of models such as Delft3D.

Ebb-tidal deltas are complex environments in both a hydrodynamic and a morphodynamic sense. Forcing conditions vary between wave- and current domination, and waves and currents can interact at different angles. Thus, traditional bedform predictors for wave-only or current-only conditions (e.g. Allen, 1968; Dingler and Inman, 1976) cannot be used. Recently, formulas were developed that incorporate both waves and currents for prediction of bedforms in mixed hydrodynamic environments (e.g. Kleinhans, 2012; Soulsby et al., 2012). However, these predictions have so far not been tested under the complex field conditions of an ebb-tidal delta.

The present study aims to analyse the spatio-temporal behaviour of small-scale bedforms on an ebb-tidal delta and relate these to the hydrodynamic forcing. The research questions are:

1. Which small-scale bedforms are present on the ebb-tidal delta?
2. How do the bedforms change through time?

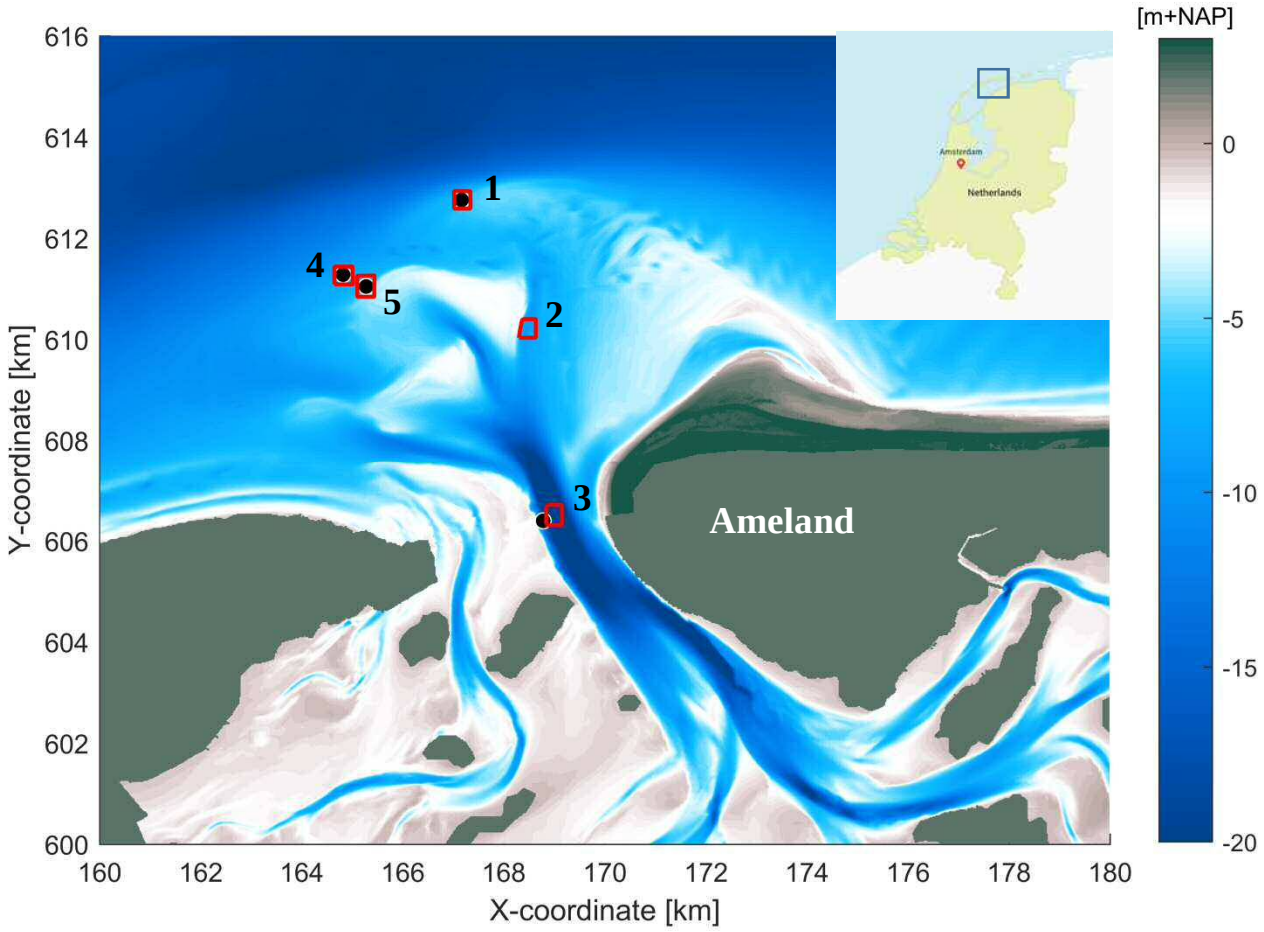

Figure 1. Bathymetry of the Ameland ebb-tidal delta of 2017 (measured by Rijkswaterstaat), including the location of multibeam measurements (red square). The measurement frames are indicated with black dots.

3. What is the relation between bedform characteristics and local hydrodynamics?

2 METHODS

The ebb-tidal delta of the Ameland Inlet, which is located in the Dutch part of the Wadden Sea, was studied in two ways. On August 29 and October 24, 2017, several parts of the ebb-tidal delta were mapped with a multibeam echo-sounder, giving an overview of bedform presence in a spatially extensive area, but at only two moments in time (Figure 1). In addition, four frames were installed in or near four of the multibeam survey areas from August 29 to September 27, 2017 (Figure 1). The frames were each equipped with a pressure transducer, three Acoustic Doppler Velocity meters (ADVs) and a Marine Electronics type 2001 3D profiling SONAR. The Sonar was mounted at 1.9 m above the bed, and set to scan the bed once per hour for approximately 15 minutes. This shows bedforms on a small spatial scale of 2x2 m, but with a high resolution in time. The measurement frequency of the pressure transducer was 4 Hz, and wave heights were calculated using the spectral moment per 30 min. Current speeds derived from the ADVs were averaged over 30 minute intervals. Grain size near frame 5 was 185.8 µm, which was determined by a box core sample.

2.1 Data analysis

The multibeam point clouds were interpolated onto a grid with 0.5x0.5 m cell size, thus eliminating small-scale ripples but still conserving the megaripples. The images

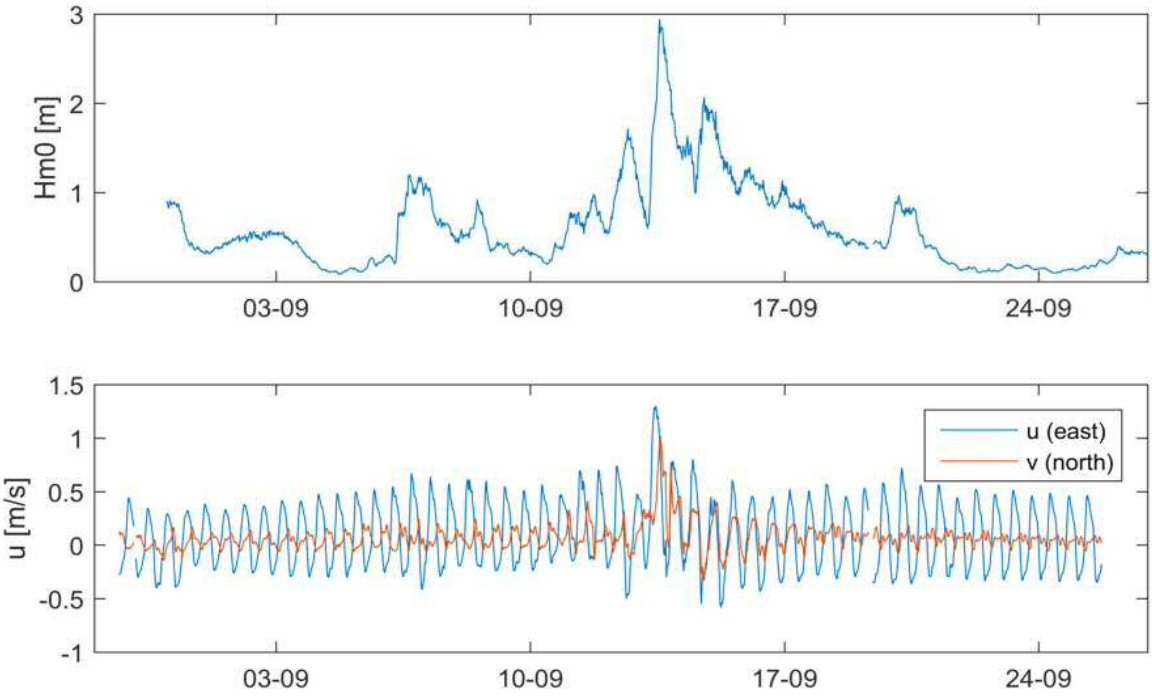

Figure 2. Wave heights and current speeds as measured at frame 5.

were processed in two ways. First, each image was divided into profiles along the x-direction, which were detrended by a second order fit. The bedform wave length L was determined by a wavelet analysis of the multibeam profiles using the method of Grindsted et al. (2004), which was based on Torrence and Compo (1998). This gives wavelengths along the profile. Combining all profiles results in a 2D image of wavelengths.

Also, the images were divided into moving windows of 25x25 m, after which the bed level in each window was detrended. Bedform heights were given by:

$$H = 2\sqrt{2}\sigma \quad (1)$$

with σ being the standard deviation of a window (Smith, 1997).

Following the bed detection procedure described in Ruessink et al. (2015), the SONAR point clouds were processed to a grid with 0.01x0.01 m cell size. Smoothing was performed with a loess filter to reveal the ripples. After a first visual inspection revealed that the ripples had length scales between 0.10 and 0.25 m, all bedforms with length scales larger than 0.42 m or smaller than 0.07 m were removed. After this, the image was detrended by subtracting a second order surface fit.

Bedform steepness was calculated as:

$$s = H/L \quad (2)$$

where H = bedform height and L = bedform wave length.

To determine bed shear stresses, wave and current related Shields parameters were calculated following Kleinhans and Grasmeijer (2006).

3 PRELIMINARY RESULTS

3.1 Hydrodynamic conditions

The wave height and current speed through time at frame 5 can be found in Figure 2. The average water depth at this frame was 6.5 m. Fair-weather conditions included wave heights between 0 and 1 m, and maximum current speeds of approximately 0.5 m/s. A storm occurred around September 13 (the maximum wave height was reached on September 13 at 13:30 hours), with wave heights up to 3 m and current speeds of

more than 1 m/s in both the u and v direction. Waves during the peak of the storm presumably broke at the frame location.

Figure 3 shows the bed shear stresses related to waves and currents, illustrating that during most of the campaign, the conditions were dominated by both waves and currents ('mixed').

3.2 Multibeam

Figure 4 shows the depth as measured by the multibeam on August 29 and October 24, together with the associated wave lengths. On August 29, bedforms with north-south oriented crests were present. These bedforms had wavelengths of 15-25 m and heights of 0.05-0.4 m, resulting in steepness values of 0.01-0.02. These megaripples (classification according to Ashley, 1990) were asymmetric, with the steeper slope pointing to the east. In contrast, no bedforms were found on October 24.

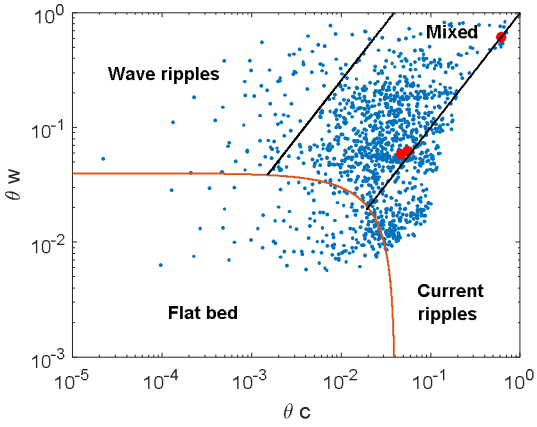

Figure 3. Nondimensional wave- (θw) and current- (θc) related Shields parameters throughout the measurement period. Red dots indicate the moments visualized in Figure 5. Black lines indicate transition between wave-, wave-current, and current-dominated ripples. Red line indicates threshold for ripples vs flat bed. (Lines reproduced after Amos et al., 1988.)

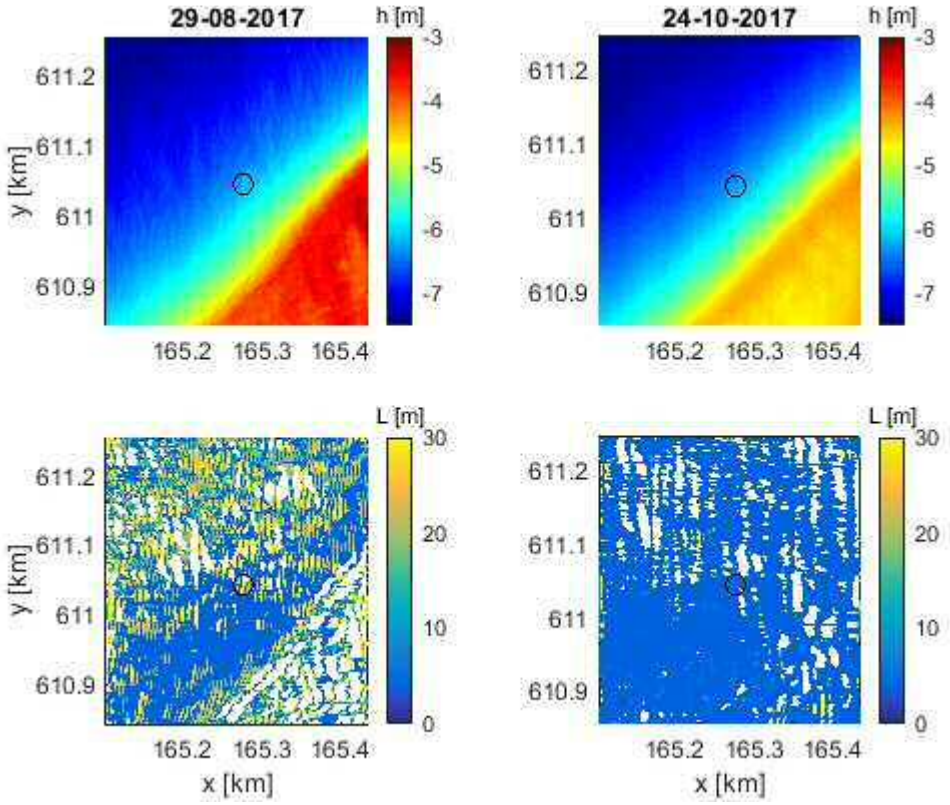

Figure 4. Depths as measured by the multibeam at August 29 (upper left) and October 24 (upper right), and the bedform wave lengths determined with wavelet analysis (bottom). Blank areas indicate that the significance was below the 95% confidence level. Circle shows the location of the frame.

It is highly likely that the storm of September 13 washed out the megaripples and also removed sand from the shoal (note the larger water depths on October 24 compared to August 29 in the lower right corner). While the storm lasted for only a few days, the megaripples were still absent six weeks later.

3.3 3D Profiling Sonar

Some typical examples of the 3D Profiling Sonar are given in Figure 5. Before and after the storm, ripples were clearly present, but no ripple crests could be defined as the images consist of disconnected three-dimensional ripples (Figure 5A and C). Ripple heights were approximately 0.05 m, and length scales were in the order of 0.1 m. In both cases, the bed state was dominated by both waves and currents, but tending towards current-dominance ($\theta_w \approx \theta_c \approx 0.05$-$0.06$). Ripples were active, i.e. their shape and position changed with time.

During the storm, the distinct ripples disappeared, but the bed never flattened out entirely (Figure 5B). The ripple marks decreased in height to less than 0.01 m. The values for the wave- and current- related Shields parameters were both 0.62, indicating that both waves and currents were highly influential (Figure 3).

Finally, it is noteworthy that the image in Figure 5C was measured just a few days after the storm and, contrary to the megaripples, clear small-scale ripples were already present again.

4 DISCUSSION

The difference between the presence of ripples and megaripples in space and time emphasizes the need of time-dependent bedform predictors for megaripples. The study area is highly dynamic and dominated by both waves and currents, which will be the basis of further research. First, ripple wave lengths and heights will be calculated, which will then be related to the wave- and current related bed shear stresses. A similar analysis will be conducted with the orientation and migration direction of all bedforms.

Future work will focus on comparing the results that were shown above to the data of the other measurement locations in Figure 1. In addition, the prediction of ripples and megaripples in both space and time will be studied.

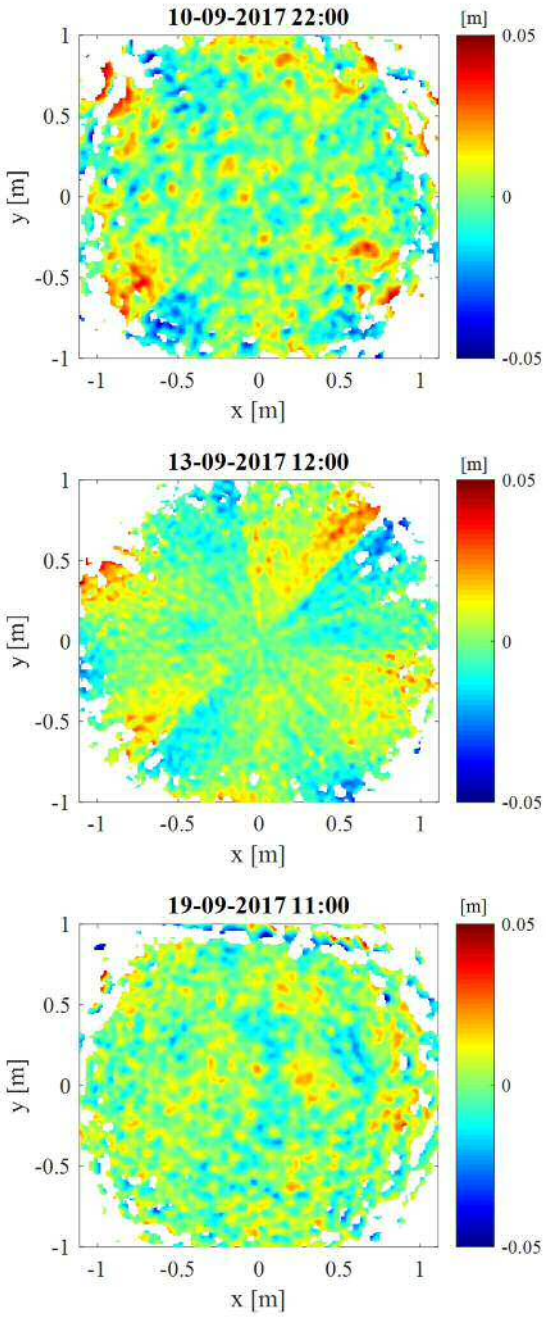

Figure 5. Bed levels as measured by the Sonar on September 10 (upper plot), 13 (middle plot) and 19 (lower plot).

5 CONCLUSIONS

At the Ameland ebb-tidal delta, small-scale 3D ripples are present most of the time, which respond quickly to changes in hydrodynamic conditions. Megaripples are not always found, suggesting that they are not only influenced by wave height and current speed, but also by the time that has passed since a storm event has taken place. Further analysis on this topic will provide more insight into the relation between hydrodynamic forcing and bedform presence and dynamics.

6 ACKNOWLEDGEMENTS

This project is part of the program SEAWAD: “SEdiment supply At the WAdden Sea ebb-tidal Delta. From system knowledge to mega-nourishments”. This research is supported by the Dutch Technology Foundation STW, which is part of the Netherlands Organisation for Scientific Research (NWO), and which is partly funded by the Ministry of Economic Affairs. The authors would like to thank Rijkswaterstaat for their support during the field campaign.

7 REFERENCES

Allen, J.R.L., 1968. Current Ripples. New York Elsevier

Amos, C.L., Bowen, A.J., Huntley, D.A., Lewis, C.F.M., 1988. Ripple generation under the combined influences of waves and currents on the Canadian continental shelf. Continental Shelf Research 8(10): 1129-1153.

Ashley, G.M., 1990. Classification of large-scale subaqeous bedforms: a new look at an old problem. Journal of sedimentary petrology 60(1): 160-172.

Brakenhoff, L.B., Van der Vegt, M., Ruessink, B.G., 2017. Saw-tooth bar dynamics on the Ameland ebb-tidal delta. Proceedings Coastal Dynamics 2017: 292-299.

Buijsman, M.C., Ridderinkhof, H., 2008. Long-term evolution of sand waves in the Marsdiep inlet. I: High-resolution observations. Continental Shelf Research 28: 1190-1201.

Dingler, J.R., Inman, D.L., 1976. Wave-formed ripples in nearshore sands. Coastal Engineering Proceedings 15: 2109-2126.

FitzGerald, D.M., 1982. Sediment bypassing at mixed energy tidal inlets. Coastal Engineering, 1094-1118.

Grinsted, A., Moore, J.C., Jevrejeva S., 2004. Application of the cross wavelet transform and wavelet coherence to geophysical time series. Nonlinear Processes in Geophysics 11: 561–566.

Hine, A., 1975. Bedform distribution and migration patterns on tidal deltas in the Chatham Harbor Estuary, Cape Cod, Massachusetts. Geology and Engineering: 235-252.

Kleinhans, M.G., 2005. Phase diagrams of bed states in steady, unsteady, oscillatory and mixed flows. EU-Sandpit end-book, Ed. Leo van Rijn, Aqua Publications, The Netherlands, paper Q

Kleinhans, M.G., Grasmeijer, B.T., 2006. Bed load transport on the shoreface by currents and waves. Coastal Engineering 53(12): 983-996. doi: 10.1016/j.coastaleng.2006.06.009

Soulsby, R.L., Whitehouse, R.J.S., Marten, K.V., 2012. Prediction of time-evolving sand ripples in shelf seas. Continental Shelf Research 38: 47-62. doi:10.1016/j.csr.2012.02.016

Ridderinkhof, W., Hoekstra, P., Van der Vegt, M., De Swart, H.E., 2016. Cyclic behaviour of sandy shoals on the ebb-tidal deltas of the Wadden Sea. Continental Shelf Research 115: 14-26.

Ruessink, B.G., Brinkkemper, J.A., Kleinhans, M.G. 2015. Geometry of wave-formed orbital ripples in coarse sand. Journal of Marine Science and Engineering 3: 1568-1594. doi: 10.3390/ jmse3041568

Smith, S.W., 1997. The Scientist and Engineer's Guide to Digital Signal Processing. California Technical Publishing San Diego, CA, USA, ISBN: 0-9660176-3-3

Torrence, C., Compo, G.P., 1998. A practical guide to wavelet analysis. Bulletin of the American Meteorological Society 79: 61–78.